Original Article

MOLECULAR METABOLISM

NR2F6 is essential for brown adipocyte differentiation and systemic metabolic homeostasis

Wei-yu Zhou [1,3], Pei Liu [1,3], Yi-fan Xia [1], Yi-jie Shi [1], Hong-yu Xu [1], Meng Ding [1], Qi-qi Yang [1], Shu-wen Qian [1], Yan Tang [1], Yan Lu [2,*], Qi-qun Tang [1,**], Yang Liu [1,*]**

ABSTRACT

Objective: Brown adipose tissue (BAT) development and function are essential for maintaining energy balance. However, the key factors that specifically regulate brown adipogenesis require further identification. Here, we demonstrated that the nuclear receptor subfamily 2 group F member 6 (NR2F6) played a pivotal role in brown adipogenesis and energy homeostasis.

Methods: We examined the differentiation of immortalized brown adipocytes and primary brown adipocytes when NR2F6 were deleted, and explored the mechanism through which NR2F6 regulated adipogenesis using ChIP-qPCR *in vitro*. Male wild type (WT) and *Pdgfra*-Cre-mediated deletion of *Nr2f6* in preadipocytes (NR2F6-PKO) mice were fed with high fat diet (HFD) for 12 weeks, and adiposity, glucose intolerance, insulin resistance and inflammation were assessed.

Results: NR2F6 exhibited abundant expression in BAT, while its expression was minimal in white adipose tissue (WAT). Within BAT, NR2F6 was highly expressed in preadipocytes, experienced a transient increase in the early stage of brown adipocyte differentiation, and significantly decreased in the mature adipocytes. Depletion of NR2F6 in preadipocytes inhibited brown adipogenesis, caused hypertrophy of brown adipocytes, and impaired thermogenic function of BAT, but without affecting WAT development. NR2F6 transcriptionally regulated PPARγ expression to promote adipogenic process in brown adipocytes. Loss of NR2F6 in preadipocytes led to increased susceptibility to diet-induced metabolic disorders.

Conclusions: Our findings unveiled NR2F6 as a novel key regulator of brown adipogenesis, potentially opening up new avenues for maintaining metabolic homeostasis by targeting NR2F6.

Keywords Brown adipose tissue; Adipogenesis; Metabolism; Nuclear receptor subfamily 2 group F member 6

1. INTRODUCTION

In mammals, white adipocytes are specialized for the storage and release of lipid, while brown adipocytes are specialized thermogenic cells that dissipate nutritional energy in the form of heat [1]. During obesity, adipose tissue expands to increase lipid storage capacity by either enlarging existing adipocytes (adipocyte hypertrophy) or generating new adipocytes (adipocyte hyperplasia) [2]. The way adipose tissue remodels strongly impacts the risk of developing metabolic disorders. Pathologic adipose tissue remodeling, typically featured by hypertrophic adipocytes, chronic inflammation, and fibrosis, is highly associated with insulin resistance [2,3]. Healthy adipose tissue expansion, characterized by adipocyte hyperplasia and the presence of smaller, numerous adipocytes, is generally linked to lower levels of inflammation and insulin resistance. Adipocyte hyperplasia refers to the adipogenic program in which preadipocytes differentiate to mature adipocytes [4]. Impaired adipogenesis, whether in white adipose tissue (WAT) or brown adipose tissue (BAT), leads to an insufficient number of adipocytes, triggers adipocyte hypertrophy, and causes ectopic lipid deposition and insulin resistance. Consequently, adipogenesis is an essential determinant of healthy adipose tissue remodeling in obesity.

[1]Key Laboratory of Metabolism and Molecular Medicine of the Ministry of Education, Department of Biochemistry and Molecular Biology of School of Basic Medical Sciences and Department of Endocrinology and Metabolism of Zhongshan Hospital, Fudan University, Shanghai 200032, China [2]Institute of Metabolism and Regenerative Medicine, Shanghai Sixth People's Hospital Affiliated to Shanghai Jiao Tong University School of Medicine, Shanghai 200233, China

[3] Wei-yu Zhou and Pei Liu contributed equally to this work.

*Corresponding author. Key Laboratory of Metabolism and Molecular Medicine, the Ministry of Education, Department of Biochemistry and Molecular Biology, Fudan University Shanghai Medical College, Shanghai 200032, China. E-mail: sudaliuyang@126.com (Y. Liu).

***Corresponding author. E-mail: luyan5011@shsmu.edu.cn (Y. Lu).

**Corresponding author. Key Laboratory of Metabolism and Molecular Medicine, the Ministry of Education, Department of Biochemistry and Molecular Biology, Fudan University Shanghai Medical College, Shanghai, 200032, China. E-mail: qqtang@shmu.edu.cn (Q.-q. Tang).

Received October 30, 2023 • Revision received January 23, 2024 • Accepted January 29, 2024 • Available online 1 February 2024

https://doi.org/10.1016/j.molmet.2024.101891

Abbreviations

BAT	brown adipose tissue
NR2F6	nuclear receptor subfamily 2 group F member 6
WAT	white adipose tissue
iWAT	inguinal white adipose tissue
eWAT	epididymal white adipose tissue
EBF2	early B-cell factor 2
PDGFRα	platelet-derived growth factor receptor-α
PRDM16	PR domain zinc finger protein 16
C/EBPβ	CCAAT/enhancer-binding protein-β
C/EBPα	CCAAT/enhancer-binding protein-α
PPARγ	peroxisome proliferator activated receptor-γ
FABP4	fatty acid binding protein 4
UCP1	uncoupling protein 1
PGC-1α	peroxisome proliferator-activated receptor gamma coactivator-1 alpha
COUP-TFs	chick ovalbumin upstream promoter-transcription factors
HFD	high fat diet
oWAT	omental white adipose tissue
SVF	stromal vascular fraction
METTL3	methyltransferase-like 3
GTT	glucose tolerance test
ITT	insulin tolerance test
SREBP	sterol regulatory element-binding protein
ChREBP	carbohydrate-responsive element-binding protein
DNL	*de novo* lipogenesis
AST	aspartate aminotransferase
ALT	alanine aminotransferase
RER	respiratory exchange ratio
ChIP	chromatin immunoprecipitation
CCK-8	cell counting kit-8
TC	total cholesterol
TG	triglyceride
FFA	free fatty acid

BAT develops before birth and enables newborns to acclimatize to the cold through non-shivering thermogenesis [4]. Brown adipocytes originate from a group of multipotent progenitor cells expressing engrailed 1, paired box 7, and myogenic factor 5 [5,6]. These progenitors first commit to brown preadipocytes that express early B-cell factor 2 (*Ebf2*) and platelet-derived growth factor receptor-α (*Pdgfra*), eventually differentiating into mature brown adipocytes [7,8]. The differentiation process of brown adipocytes is tightly regulated by multiple transcription factors and cofactors such as PR domain zinc finger protein 16 (PRDM16), EBF2, CCAAT/enhancer-binding protein-β (C/EBPβ), CCAAT/enhancer-binding protein-α (C/EBPα), peroxisome proliferator activated receptor-γ (PPARγ), zinc finger protein 516, and euchromatic histone-lysine N-methyltransferase 1 [9–11]. Cold exposure stimulates the proliferation of brown preadipocytes and promotes their *de novo* differentiation into mature brown adipocytes [12]. The quantity of brown adipocytes is highly associated with metabolic health, making the identification of regulators that promote brown adipocyte differentiation potentially valuable for intervention in metabolic disorders.

Chick ovalbumin upstream promoter-transcription factors (COUP-TFs) are a group of orphan receptors, which include COUP-TFIII (also known as nuclear receptor subfamily 2 group F member 6 or NR2F6), COUP-TFI (also known as NR2F1) and COUP-TFII (also known as NR2F2) [13]. NR2F6 is a key transcription factor that plays a role in regulating tumorigenesis, immunity, metabolic process and neuron function [14–16]. In our previous study, we demonstrated that NR2F6 promotes fatty acid uptake in the liver, resulting in hepatic steatosis and insulin resistance [16]. However, the function of NR2F6 in brown fat has not been elucidated yet. In the current study, we found that NR2F6 had an abundant expression in the preadipocytes of BAT. *Pdgfra*-Cre-mediated deletion of *Nr2f6* in preadipocytes (NR2F6-PKO) inhibited brown adipocyte differentiation and subsequently led to hypertrophy and impaired function of BAT. Consequently, the loss of *Nr2f6* aggravated high fat diet (HFD)-induced obesity and metabolic disorders.

2. MATERIAL AND METHODS

2.1. Animal model

All WT C57BL/6J mice and *Nr2f6*$^{flox/flox}$ mice were purchased from Gempharmatech Co., Ltd (Nanjing, China). *Pdgfra-Cre* mice were generously provided by Prof. Tong-jin Zhao from Fudan university [17]. B6.Cg-*Gt(ROSA)26Sor*$^{tm9(CAG-tdTomato)Hze}$/J (R26-LSL-tdTomato; stock no. 007909) were purchased from the Jackson Laboratory [18]. *Nr2f6*$^{flox/flox}$ mice, containing loxp sites flanking exon 2 of the *Nr2f6* gene, were generated using CRISPR-Cas9 technology. Preadipocytes specific *Nr2f6* knockout mice (NR2F6-PKO) were obtained by crossing *Nr2f6*$^{flox/flox}$ mice with *Pdgfra-Cre* mice. The mice were housed at 21 ± 1 °C with a humidity of 50 % ± 5 %, unless otherwise specified, with a 12-hour light–dark cycle with ad libitum access to food and water. Chow diets were purchased from Shanghai Pulutong Biotechnology (P1101F). For diet-induced obesity studies, mice were fed with HFD (D12492, 60 % fat, Research Diets, Inc). Body weights of these mice were measured weekly. Body fat and lean mass were quantified using an NMR analyzer (Minispec LF90II; Bruker Optics). All studies involving animal experiments were approved by the Fudan University Shanghai Medical College Animal Care and Use Committee (No. 20230301-045) and followed the National Institutes of Health guidelines on the care and use of animals.

2.2. Animal metabolic measurements

Mice were housed individually in metabolic cages (CLAMS; Columbus Instruments, Columbus, OH, USA) and free access to food and water. Oxygen consumption, carbon dioxide production, respiratory exchange ratio (RER) and heat were monitored for 72 h, during light and dark cycles.

2.3. Cell culture

SVF cells from adipose tissues were fractionated by collagenase digestion (Sigma–Aldrich, Cat# C2139) and plated in culture according to the methods described previously [19,20]. SVF cells were cultured in Dulbecco's modified Eagle medium (DMEM; Gibco, Cat# 11995065) containing 10 % fetal bovine serum (FBS; Gibco, Cat# 10091-148). For differentiation assays, confluent preadipocytes (designated day 0) were treated with a medium containing 10 % FBS, 0.5 mM isobutylmethylxanthine, 125 nM indomethacin, 1 mM dexamethosone, 1 μg/mL insulin, and 1 nM T3 until day 2. The cells were then maintained in media containing 10 % FBS, 1 μg/mL insulin, 1 nM T3 and until ready for harvest (generally day 6–7 post differentiation). DE-2-3 immortalized brown preadipocytes were generated as previously described [21], and cultured with DMEM containing 10 % FBS. Upon

reaching 70 % confluence (designated −2 day), brown preadipocytes were induced to differentiate into brown adipocytes with differentiation medium (DMEM containing 10 % FBS, 1 μg/mL insulin, and 1 nM T3) until day 0. Cells then received induction medium (DMEM containing 10 % FBS, 1 μg/mL insulin, 1 nM T3, 0.5 mM isobutylmethylxanthine (IBMX), 0.5 μM dexamethasone, and 0.125 mM indomethacin) for 2 days, after which cells were fed differentiation medium, which was changed every other day. Cells were fully differentiated and expressed high levels of uncoupling protein 1 (UCP1) on day 6.

2.4. RNA interference assay

To knock down NR2F6, the cells were seeded into 3.5 cm dishes and transfected with siRNA at 70 % confluence as previously described [22]. Briefly, siRNAs and RNA iMAX transfection reagent were separately diluted in Opti-minimal essential medium (MEM). The diluted siRNAs were added to the diluted RNA iMAX transfection reagent and incubated for 20 min. Next, the siRNA mixture was slowly added to the cells. After 12—24 h, the transfection medium was replaced with normal culture medium, and subsequent experiments were performed 48 h after transfection. The following sequences for siRNA were used: siNC (5′-UUCUCCGAACGUGUCACGUTT-3′; 5′-ACGUGACACGUUCGGAGAATT-3′), si*Nr2f6*-1 (5′-GGGACAAGUCCAGUGGAAAGCAUUA-3′; 5′-UAAUGCUUUCCACUGGACUUGUCCC-3′) and si*Nr2f6*-2 (5′-CAUCCCUCAUCUCCCAGCUCUUCUU-3′; 5′-AAGAAGAGCUGGGAGAUGAGGGAUG-3′).

2.5. Generation of recombinant adenovirus

The generation of recombinant adenovirus (Ad) for NR2F6 overexpression was carried out using the ViraPower Adenoviral Expression System (Invitrogen, Carlsbad, CA) as previously described [23,24]. A LacZ recombinant adenovirus was utilized as the negative control. Recombinant Ad was produced and amplified in 293A cells and purified using Ad purification kits (Sartorius, Göttingen, Germany). The purified Ad was then used to transfect preadipocytes, which were subsequently subjected to the adipogenic process.

2.6. Cold tolerance test

Cold tolerance test was conducted as previously described [23]. In cold exposure experiments, mice were placed in prechilled cages set at 4 °C with unrestricted access to water and food. Rectal temperature was measured using an animal electronic thermometer (Alcott Biotech, Shanghai, China) at the indicated times after cold exposure.

2.7. Oil red O staining and BODIPY staining

The cells were first washed thrice with phosphate-buffered saline (PBS) and subsequently fixed for 10 min in 3.7 % formaldehyde. Cells were then washed with water and stained with oil red O working solution overnight at room temperature. For BODIPY staining, differentiated cells were washed with PBS, fixed with 4 % paraformaldehyde for 20 min at room temperature, and stained with BODIPY (LD02, Dojindo) for 10 min. Finally, the cells were photographed using a microscope and subjected to analysis.

2.8. RT-PCR analysis

Total RNA was extracted using TRIzol reagent (Thermo Fisher Scientific, Cat# 15596018) and dissolved in diethyl pyrocarbonate water. Reverse transcription was performed with 500 ng of total RNA using the TaKaRa Reverse Transcription Kit (TaKaRa Bio, Otsu, Japan, Cat# RR047A). Using a ChamQ Universal SYBR qPCR Master Mix (Vazyme, Cat# Q711-02) and complementary DNA as the template, the target fragment was amplified by adding specific primers of the gene of interest. The expression levels of the genes were determined by the fluorescence intensity of the target fragment. Each reaction was performed in triplicate. Relative mRNA levels were calculated according to the Ct value, and the Ct value of 18s rRNA was used for normalization. Primers for quantitative RT-PCR are shown in Supplemental Table 1.

2.9. Western blot

The tissues or cells were lysed and denatured at 100 °C for 10 min. The protein concentration was determined using the bicinchoninic acid assay. Equal amounts of protein were separated by SDS-PAGE, transferred to a polyvinylidene difluoride membrane (Millipore Corp), and immunoblotted overnight at 4 °C with the following primary antibodies: NR2F6 (Abcam; ab137496), PPARγ (Cell Signaling Technology; 81B8), PGC-1α (Proteintech; 66369-1-Ig), Flag tag (Sigma—Aldrich; F1804), UCP1 (Abcam; ab10983), C/EBPα (Santa Cruz; sc-365318) (422/aP2 antibody was kindly provided from M. Daniel Lane). After washing three times, the membranes were further incubated with the corresponding HRP-conjugated secondary antibodies (Jackson ImmunoResearch) for 1 h at room temperature. Protein bands were visualized using a chemiluminescence detection kit (ShareBio, Cat# SB-WB012) and analyzed with a luminescent ImageQuant LAS 4000 image analyzer (GE Healthcare Life Sciences).

2.10. Glucose tolerance tests and insulin tolerance tests

In the glucose tolerance test experiment, HFD-fed mice were fasted overnight before being injected intraperitoneally with a D-glucose solution (1.5 g/kg body weight). In the insulin tolerance test experiment, mice fasted for 6 h and then were injected intraperitoneally with a human insulin solution (0.75 mU/g body weight). Tail blood glucose concentration was measured at 0, 15, 30, 60, 90 and 120 min after injection of glucose or insulin by using a glucometer (Accu-Chek; Roche).

2.11. Dual luciferase reporter assay

HEK-293T cells were transfected with 250 ng of pGL3-basic vector containing the *Pparg2* promoter, Renilla vector, and *Nr2f6* expression plasmids using Hieff Trans Liposomal Transfection Reagent (Yeasen) in 24-well plates. After 36 h post-transfection, the cells were lysed and their luciferase activity was measured using the Dual Luciferase Reporter Assay System (Promega, Cat# E1910).

2.12. Chromatin immunoprecipitation (ChIP)

Immortalized brown adipocytes overexpressed with Flag-NR2F6 were subjected to ChIP assay. After post-adipogenic induction, mature brown adipocytes were cross-linked in 1 % Formaldehyde at room temperature for 10 min and then incubated with 2.5 M Glycine for 5 min to terminate cell fixation. The cells were resuspended in lysis buffer (50 mM HEPES pH 7.5, 140 mM NaCl, 2 mM EDTA, 0.1 % Na-Deoxycholate, and 0.1 % SDS) with protease inhibitor after being washed 3 times with ice-cold PBS, and were incubated on ice for 10 min. Then, the lysates were mixed well and sonicated by Bioruptor (Diagenode), and the length of DNA fragments ranged between 200 and 600 bp. After centrifugation, the cell lysates were diluted in ChIP lysis buffer with protease inhibitor, and 50 μL of the sample was used for input control. The diluted lysates were immunoprecipitated with the Flag antibody (Sigma, Cat# F1804-1MG) overnight at 4 °C. The immune complexes were then incubated by ChIP Grade Protein A/G magnetic beads (Thermo Fisher, Cat#26162) for 2 h at 4 °C, and were washed with washing buffer (500 mM LiCl, 50 mM HEPES, pH 7.5, 1 mM EDTA, 0.1 % Na-Deoxycholate, and 1 % NP40) for 5 times, followed by TE buffer (10 mM Tris—HCl, pH 8.0, and 1 mM EDTA) and

then eluted with ChIP elution buffer (50 mM Tris—HCl, pH 8.0, 10 mM EDTA, and 1 % SDS). The input and immunoprecipitated DNA were reverse cross-linked, followed by protein kinase at 65 °C for 16 h, and purified using a Cell/Tissue DNA Isolation Mini Kit (Vazyme, Cat# DC102-01). The DNA was analyzed by real-time qPCR through the ViiA 7 Real-Time PCR System (Applied Biosystems) in technical triplicates. Target enrichment was calculated as percent input and normalized to control. Primers were as follows: Pparg, 5′-TAGTCCCCTTGAAGAATGAATAGTTACT-3′ and 5′-CCTCCCTGAGAA-TAATGTATTACCAGAA-3′.

2.13. Cell counting kit-8 (CCK-8)

Cells were seeded into 96-well microplates. After culture for 4 h, 10 μL of CCK-8 reagent (Yeasen, Cat# 40203ES60) was added to each well and then cultured for 2 h. The absorbance was analysed at 450 nm using a microplate reader.

2.14. Free fatty acid (FFA) and insulin detection

The concentrations of FFA (Solarbio, Cat# BC0595) were determined using the corresponding kits as indicated in their instructions. Insulin was determined by ELISA (CrystalChem, Cat# 90080), according to the manufacturer's instructions.

2.15. Statistical analysis

GraphPad Prism 8.0 software (GraphPad Software, San Diego, CA, USA) was used for statistical analysis. All data are shown as the mean ± SD. Two-tailed unpaired Student's t-test was used to compare two groups with normally distributed data. Two-tailed unpaired Student's t-test with Welch's correction was used for two groups with unequal variances. Mann—Whitney test was used to compare two groups without normal distribution. To compare more than two groups, one-way ANOVA with Bonferroni test was used to analyze normally distributed data; Brown-Forsythe and Welch ANOVA tests followed by Tamhane's T2 multiple comparisons test was used to compare more than two groups with unequal variances; nonparametric statistical analysis for the data without a normal distribution was performed using the Kruskal—Wallis test with Dunn's test for multiple comparisons. Two-way ANOVA followed by Bonferroni's multiple comparisons test was used for comparison between multiple groups with two fixed factors, with $p < 0.05$ considered statistically significant. Statistical analysis used in each panel was described in the figure legends.

3. RESULTS

3.1. NR2F6 is abundantly expressed in BAT

To determine the expression of NR2F6, we examined the mRNA and protein levels of NR2F6 in various adipose tissues from 8-week-old male C57BL/6J mice. We found that *Nr2f6* exhibited higher mRNA levels in BAT compared to inguinal WAT (iWAT) or epididymal WAT (eWAT) (Figure 1A). The protein expression of NR2F6 was found to be abundant in BAT, while its expression in iWAT or eWAT was weak and negligible (Figure 1B). To further validate these findings, we compared gene expression profiles of human fetal BAT and adult omental WAT (oWAT) using publicly available gene expression data. In concert with the mouse data, *Nr2f6* was highly enriched in human fetal BAT compared with oWAT (Figure 1C). Moreover, NR2F6 showed predominant expression in the stromal vascular fraction (SVF) rather than mature adipocytes in BAT (Figure 1D). During adipogenic differentiation in immortalized brown preadipocytes, NR2F6 exhibited high expression in preadipocytes, but its expression sharply decreased on day 2 post-adipogenic induction and remained low in mature adipocytes

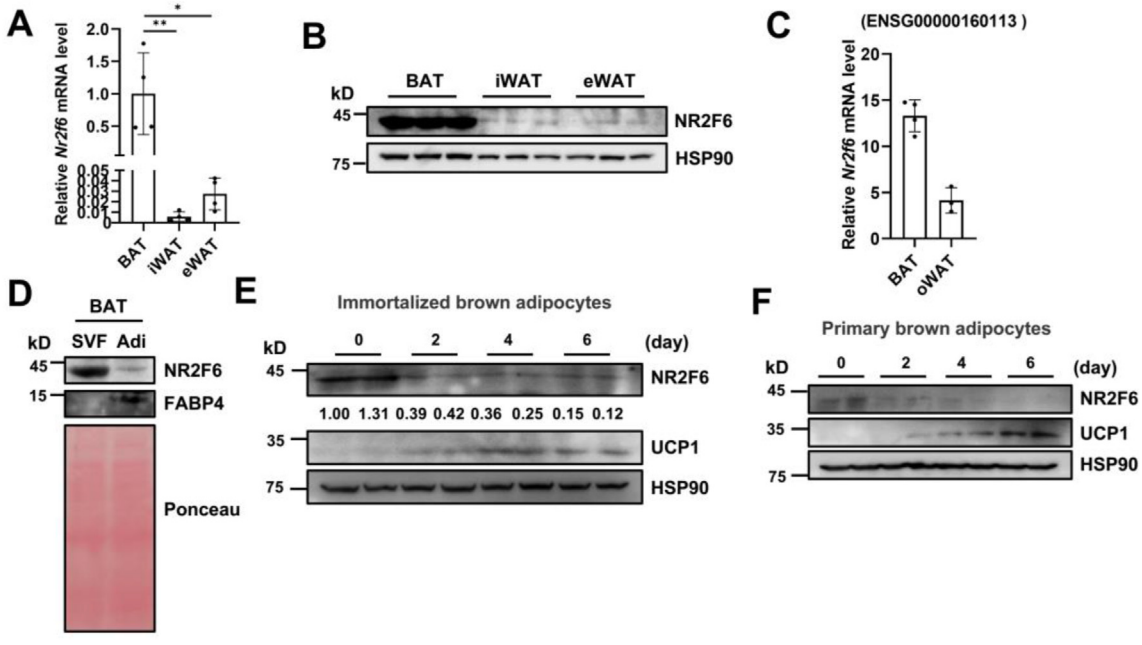

Figure 1: NR2F6 is expressed abundantly in brown adipose tissue (BAT). (A) Relative *Nr2f6* mRNA levels in BAT, inguinal WAT (iWAT) and epididymal WAT (eWAT) of 8-week-old male C57BL/6J mice (n = 4). (B) Relative NR2F6 protein levels in BAT, iWAT and eWAT of 8-week-old male C57BL/6J mice (n = 3). (C) Relative *Nr2f6* mRNA levels in human fetal BAT and adult omental WAT (oWAT) from the publicly available gene expression database. (D) Relative NR2F6 protein levels in isolated stromal vascular fraction (SVF) and mature adipocytes from BAT of 8-week-old male C57BL/6J mice. (E) Relative NR2F6 protein levels during the time course of immortalized brown adipocyte differentiation. (F) Relative NR2F6 protein levels during the time course of primary brown adipocyte differentiation. Data are represented as mean ± SD. Data in A was analyzed by one-way ANOVA. *$p < 0.05$, **$p < 0.01$, ***$p < 0.001$.

(Figure 1E). We observed similar expression trend of NR2F6 during adipogenic differentiation in isolated SVF from BAT (Figure 1F). We also found that cold exposure for 72 h could increase *Nr2f6* expression in BAT SVF and the number of *Nr2f6* positive expressing preadipocytes but not in iWAT SVF (Figure S1A–C). These results indicated that NR2F6 was highly expressed in preadipocytes of BAT and significantly decreased in the mature adipocytes.

3.2. Deficiency of NR2F6 leads to impairment in brown fat

Since NR2F6 was highly expressed in preadipocytes, we generated mice with depleted *Nr2f6* specifically in preadipocytes (NR2F6-PKO) by crossing *Nr2f6*$^{flox/flox}$ mice with *Pdgfra*-Cre mice, a widely recognized Cre transgenic mouse tool for targeting preadipocytes [25]. Both the protein and mRNA levels of NR2F6 were dramatically decreased in preadipocytes of BAT from NR2F6-PKO mice (Figure 2A,B). We did not observe a reduction in NR2F6 expression in preadipocytes of iWAT or eWAT from NR2F6-PKO mice (Figure S2A–D), possibly due to its lower expression in these tissues. On postnatal day 3, there were no differences in body weight, fat mass, or gross morphology of adipose tissue between NR2F6-PKO mice and WT littermates (Figure S3A–C). However, general adipogenic markers, including PPARγ, fatty acid binding protein 4 (FABP4) and the BAT-specific marker UCP1, were dramatically decreased in BAT of NR2F6-PKO mice (Figure 2C,D). In adult mice, BAT mass was identical between WT and NR2F6-PKO mice (Figure 2E), whereas H&E staining revealed increased lipid deposition and a transition from small to large lipid droplets in BAT of NR2F6-PKO

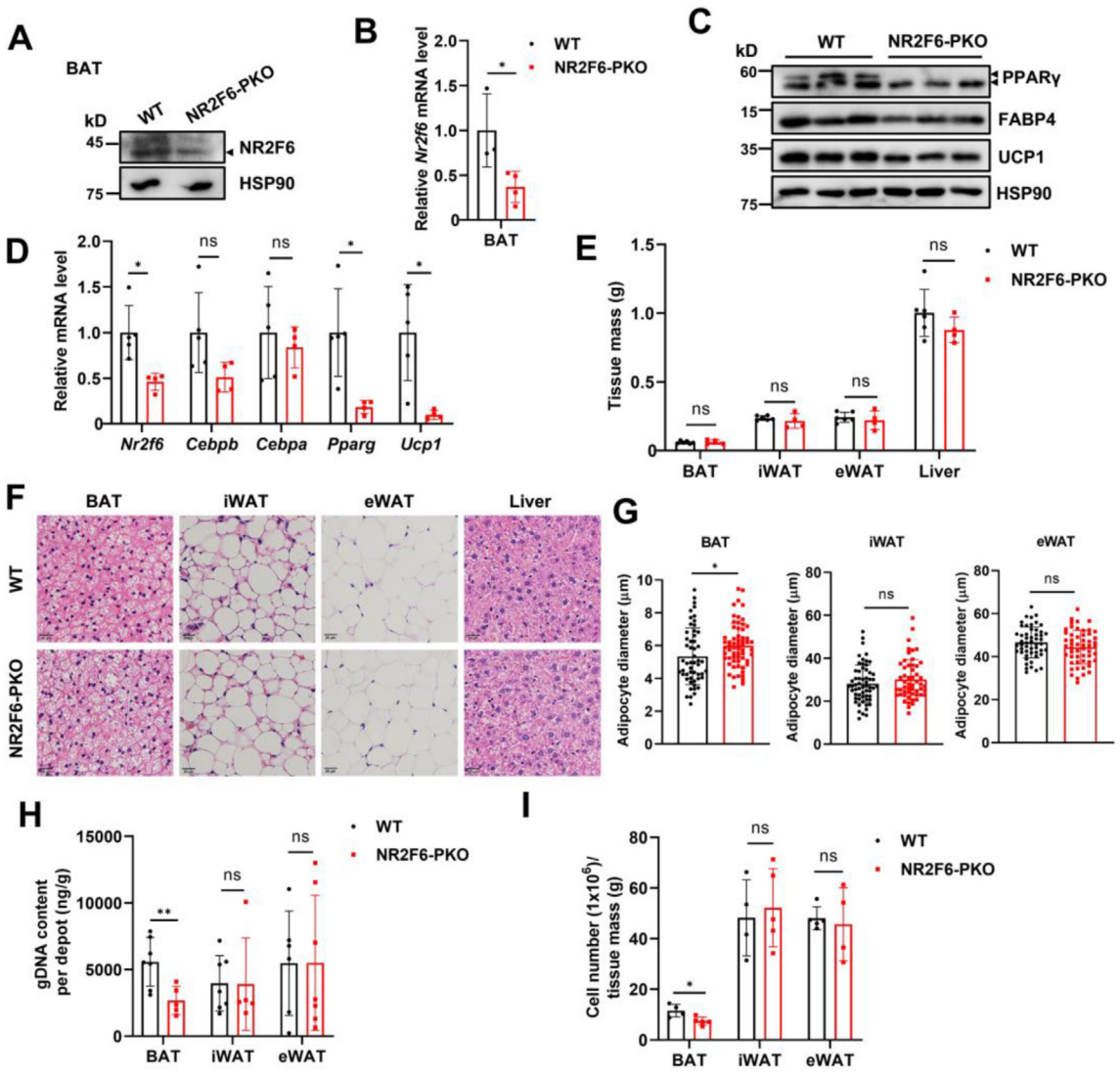

Figure 2: *Nr2f6* deficiency in preadipocytes induces hypertrophy of brown adipocytes. (A) Relative protein levels of NR2F6 in preadipocytes of BAT from 6-week-old WT and NR2F6-PKO mice. (B) Relative mRNA levels of *Nr2f6* in preadipocytes of BAT from 6-week-old WT and NR2F6-PKO mice (WT mice, n = 3; NR2F6-PKO mice, n = 4). (C) Relative protein levels of PPARγ, FABP4, and UCP1 in BAT of postnatal day 3 WT and NR2F6-PKO mice (n = 3). (D) Relative mRNA levels of *Nr2f6*, adipogenesis markers (*Cebpb*, *Cebpa*, and *Pparg*) and brown adipocyte marker (*Ucp1*) in BAT of postnatal day 3 WT and NR2F6-PKO mice (WT mice, n = 5; NR2F6-PKO mice, n = 4). (E) The tissue mass of 8-week-old WT and NR2F6-PKO mice (WT mice, n = 6; NR2F6-PKO mice, n = 4). (F) H&E staining of BAT, iWAT, eWAT, and liver of 8-week-old WT and NR2F6-PKO mice. Scale bar, 20 μm. (G) Adipocyte diameter of BAT, iWAT, and eWAT of 8-week-old WT and NR2F6-PKO mice (adipocytes in BAT of WT mice, n = 53; adipocytes in BAT of NR2F6-PKO mice, n = 62; adipocytes in iWAT of WT mice, n = 59; adipocytes in iWAT of NR2F6-PKO mice, n = 53; adipocytes in eWAT of WT mice, n = 52; adipocytes in eWAT of NR2F6-PKO mice, n = 53). (H) Genomic DNA content of mature adipocytes per fat depot (WT mice, n = 6–7; NR2F6-PKO mice, n = 5–7). (I) The number of mature adipocytes per fat depot (n = 4–5). Data are represented as mean ± SD. Data in B, D, E, G, H, and I were analyzed by Student's t-test. *p < 0.05, **p < 0.01, ***p < 0.001.

mice (Figure 2F,G). In contrast, both the total tissue mass and the size of adipocytes in WAT remained unchanged (Figure 2E—G). The hypertrophy of brown adipocytes without changes in the overall volume of fat pads suggested a possible decrease in the number of mature adipocytes. Indeed, the number of adipocytes in BAT of NR2F6-PKO mice was significantly reduced (Figure 2H,I).

We then conducted cold tolerance test to assess the thermogenic capacity of NR2F6-PKO mice. We first performed WT and NR2F6-PKO mice with food under cold exposure for 72 h, and found that NR2F6-PKO mice had the similar core body temperature with WT mice (Figure S4A). In fasted state, the body temperature of NR2F6-PKO mice was obviously lower than WT mice (Figure 3A). NR2F6-PKO mice exhibited a hypertrophic feature of brown adipocytes under cold exposure (Figure 3B). The expression levels of thermogenesis-related markers such as UCP1 and peroxisome proliferator-activated receptor gamma coactivator-1 alpha (PGC-1α) were significantly decreased in both mRNA and protein levels in the BAT of NR2F6-PKO mice (Figure 3C,D), while these genes in iWAT remained unchanged in 24 h cold exposure (Figure 3E). In addition, for long time cold exposure (72 h), no significant difference in the expression of thermogenesis gene in iWAT was observed (Figure S4B). These data together indicated that NR2F6-PKO mice exerted impaired thermogenic function in BAT.

3.3. NR2F6 is essential for the differentiation of brown adipocytes

Upon observing a decrease in the number of brown adipocytes in NR2F6-PKO mice, we then investigated whether NR2F6 regulated brown adipocyte differentiation. We obtained the SVF from BAT of WT and NR2F6-PKO mice on postnatal day 3 and induced adipogenesis. Strikingly, depletion of *Nr2f6* in preadipocytes dramatically inhibited adipogenesis process, as evidenced by a decrease in BODIPY staining for lipid droplets (Figure 4A). The expressions of general adipogenesis markers (*Pparg, Cebpa, Adiponectin,* and *Fabp4*) as well as brown adipocyte markers (*Ucp1* and *Pgc1a*) were significantly decreased (Figure 4B,C). We also examined the expression of sterol regulatory element-binding protein (SREBP) and carbohydrate-responsive element-binding protein (ChREBP) in primary brown adipocytes of P3 WT and NR2F6-PKO mice. The mRNA of *Chrebpa*, *Chrebpb*, *Srebf1a*, and *Srebf1c* were not altered (Figure S5A). Subsequently, we disrupted *Nr2f6* expression in immortalized brown preadipocytes using two sets of si*Nr2f6* and observed that *Nr2f6* deficiency potently inhibited the formation of mature adipocytes and downregulated the expression of *Pparg*, *Cebpa*, *Pgc1a*, *Adiponectin*, *Fabp4*, and *Ucp1* (Figure 4D—F). To complement the loss-of-function model of *Nr2f6*, we isolated SVF of BAT and overexpressed *Nr2f6* in the preadipocytes by infecting the cells with Ad-NR2F6. Consistent with the observation that loss of NR2F6 inhibited adipogenesis, *Nr2f6* overexpression promoted adipogenic differentiation as indicated by increased BODIPY and oil Red O staining, and increased expression of PPARγ, FABP4, and UCP1 (Figure 4G,H). As expected, *Nr2f6* overexpression in iWAT SVF also promoted the expression of thermogenic genes, including *Ucp1* and *Pgc1a* (Figure S5B). To understand the precise function of NR2F6 during adipogenesis *in vivo*, we crossed NR2F6-PKO mice with R26-loxP-stop-loxP-tdTomato mice to generate NR2F6-PKO; R26-tdTomato mice, which tagged mature adipocytes derived from PDGFRα$^+$ progenitors by using tdTomato. Our strategy for lineage tracing showed that BAT had fewer new adipocytes derived from PDGFRα$^+$ progenitors in NR2F6-PKO; R26-tdTomato mice (Figure 4I,J). In addition to regulate adipogenesis, we also found that NR2F6 might modulate the proliferation of progenitor cells, as indicated by the Cell Counting Kit-8 (CCK-8) assay (Figure S6A and B).

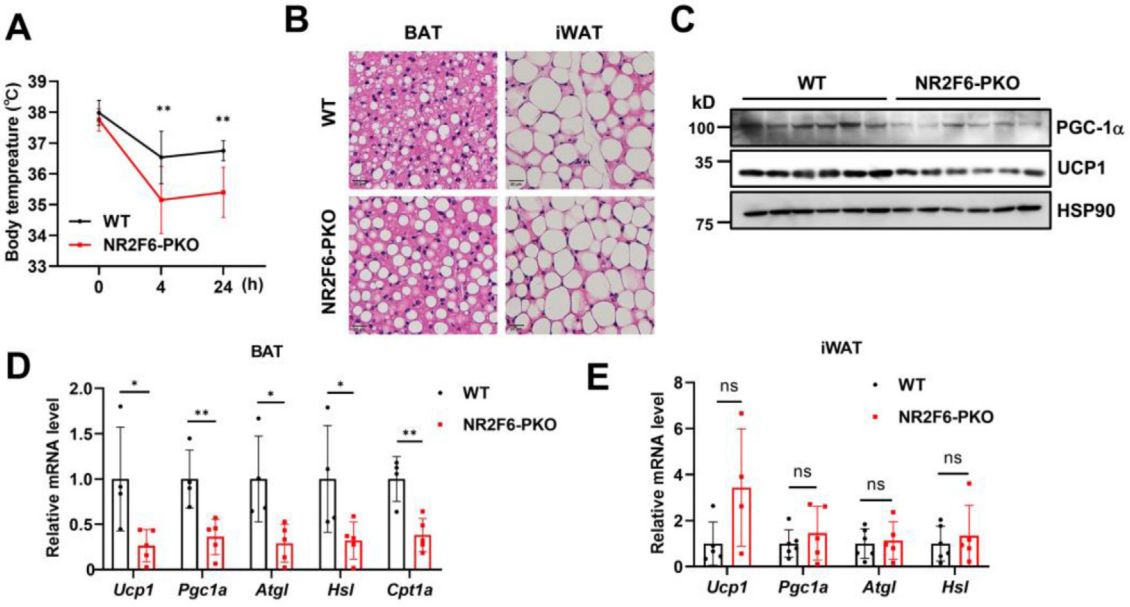

Figure 3: Loss of *Nr2f6* inhibits thermogenic capacity of BAT. (A) Changes in rectal temperature during 4 °C cold exposure under 24 h fasting conditions (n = 6). (B) H&E staining of BAT and iWAT of 8-week-old WT and NR2F6-PKO mice after exposure at 4 °C for 24 h upon fasting. Scale bar, 20 μm. (C) Relative protein levels of thermogenic-related markers (PGC-1α and UCP1) in BAT of 8-week-old WT and NR2F6-PKO mice after exposure at 4 °C for 24 h upon fasting (n = 6). (D) Relative mRNA levels of thermogenic-related markers (*Pgc1a* and *Ucp1*), lipolysis markers (*Atgl* and *Hsl*) and fatty acid oxidation marker (*Cpt1a*) in BAT of 8-week-old WT and NR2F6-PKO mice after exposure at 4 °C for 24 h upon fasting (WT mice, n = 4; NR2F6-PKO mice, n = 5). (E) Relative mRNA levels of thermogenic-related markers (*Pgc1a* and *Ucp1*) and lipolysis markers (*Atgl* and *Hsl*) in iWAT of 8-week-old WT and NR2F6-PKO mice after exposure at 4 °C for 24 h upon fasting (WT mice, n = 5—6; NR2F6-PKO mice, n = 4—6). Data are represented as mean ± SD. Data in A was analyzed by two-way ANOVA. Data in D and E were analyzed by Student's t-test. *p < 0.05, **p < 0.01, ***p < 0.001.

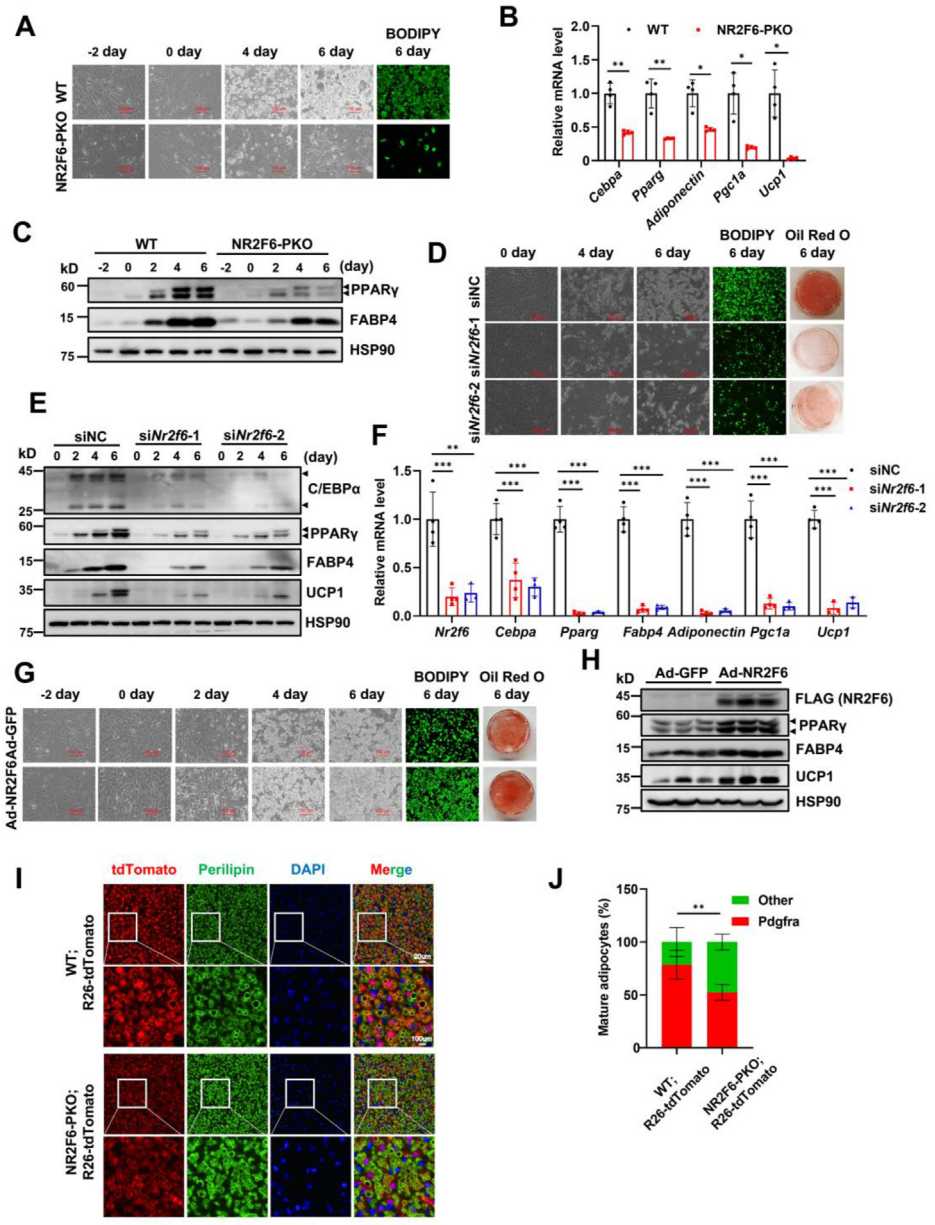

Figure 4: Deletion of *Nr2f6* blocks adipogenic differentiation. (A–C) SVF cells were isolated from BAT of P3 WT and NR2F6-PKO mice and subjected to adipogenic induction. (A) Brightfield images and BODIPY staining showing adipogenesis in primary brown adipocytes. Scale bar, 100 μm. (B) Relative mRNA levels of adipogenesis markers (*Cebpa, Pparg,* and *Adiponectin*) and brown adipocyte markers (*Pgc1a* and *Ucp1*) on day 6 of adipocyte differentiation (n = 4). (C) Relative protein levels of PPARγ and FABP4 during adipocyte differentiation. (D–F) Immortalized brown adipocytes treated with siNC or si*Nr2f6* were subjected to adipogenic differentiation. (D) Brightfield images, oil red O staining, and BODIPY staining showing the adipogenesis. Scale bar, 100 μm. (E) Relative protein levels of adipogenesis markers (C/EBPα, PPARγ, and FABP4) and brown adipocyte marker (UCP1) during the adipocyte differentiation. (F) Relative mRNA levels of adipogenesis markers (*Cebpa*, *Pparg*, *Fabp4*, and *Adiponectin*) and brown adipocyte markers (*Pgc1a* and *Ucp1*) on day 6 of adipocyte differentiation (n = 3–4). (G–H) SVF cells were isolated from BAT of P3 C57BL/6J mice and treated with Ad-GFP or Ad-NR2F6. (G) Brightfield images, oil red O staining, and BODIPY staining showing the adipogenesis. Scale bar, 100 μm. (H) Relative protein levels of adipogenesis markers (PPARγ and FABP4) and brown adipocyte marker (UCP1). (I–J) NR2F6-PKO mice were crossed with R26-loxP-stop-loxP-tdTomato mice to generate NR2F6-PKO; R26-tdTomato mice. Mature adipocytes derived from PDGFRα$^+$ progenitors labeled by tdTomato. (I) Immunofluorescent staining for BAT of 4-week-old WT; R26-tdTomato mice and NR2F6-PKO; R26-tdTomato mice. Representative images of BAT sections stained with tdTomato, Perilipin, and DAPI. Scale bars, 20 μm and 100 μm. (J) Quantification of the percentage of mature adipocytes derived from PDGFRα$^+$ progenitors (n = 6). Data are represented as mean ± SD. Data in B and J were analyzed by Student's t-test. Data in F was analyzed by one-way ANOVA *p < 0.05, **p < 0.01, ***p < 0.001.

We proceeded to investigate the mechanism through which NR2F6 regulated adipogenesis. Since NR2F6 deficiency led to downregulation of PPARγ, we speculated whether NR2F6 regulated the transcription of *Pparg*. To explore this, we examined the expression of NR2F6 over time during the differentiation of immortalized brown adipocytes. Interestingly, NR2F6 protein levels peaked at 8 h after adipogenic induction, gradually declined thereafter, and maintained low in mature adipocytes (Figure 5A). Concurrently, we observed a rapid elevation of *Pparg* mRNA levels at 8 h after adipogenic induction (Figure 5B). Utilizing JASPAR database, we predicted a potential binding site for

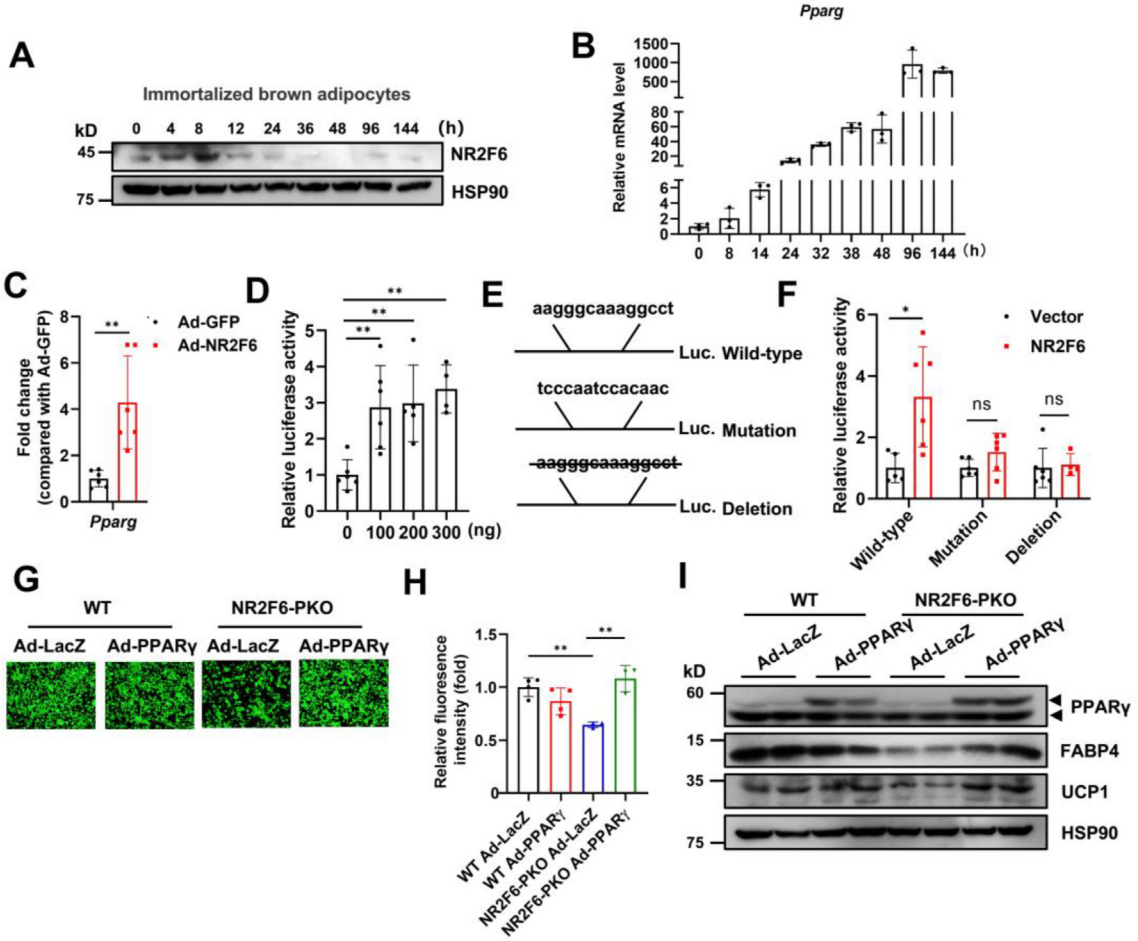

Figure 5: NR2F6 transcriptionally activates PPARγ to promote adipocyte differentiation. (A) Relative NR2F6 protein levels during immortalized brown adipocyte differentiation. (B) Relative *Pparg* mRNA levels during immortalized brown adipocyte differentiation (n = 3). (C) ChIP-qPCR analysis showing the binding of NR2F6 to the *Pparg* promoter (n = 6). (D) Luciferase activity of *Pparg* promoter regulated by NR2F6 (n = 4–6). (F) Illustration of wild-type, mutation or deletion of the predicted binding site of the *Pparg* promoter for NR2F6. (F) Luciferase activity of *Pparg* promoter reporter (Control vector, n = 5–6; NR2F6 vector, n = 4–6). (G–I) SVF isolated from BAT of P3 WT and NR2F6-PKO mice were overexpressed with PPARγ and subjected to adipogenic induction. (G) BODIPY staining of adipocytes on day 6 after differentiation. (H) Relative fluorescence intensity of adipocytes on day 6 after differentiation (n = 3–4). (I) Relative protein levels of adipogenesis markers (PPARγ and FABP4) and brown adipocyte marker (UCP1) were detected on day 6 of adipocyte differentiation. Data are represented as mean ± SD. Data in C and F were analyzed by Student's t-test. Data in D and H were analyzed by one-way ANOVA. *p < 0.05, **p < 0.01, ***p < 0.001.

NR2F6 on the promoter region of *Pparg*. ChIP-qPCR confirmed the binding of NR2F6 to *Pparg* promoter (Figure 5C). Furthermore, luciferase reporter analysis showed that NR2F6 activated the promoter activity of *Pparg* (Figure 5D). Notably, deletion or mutation of the predicted NR2F6 binding site significantly diminished the luciferase activity (Figure 5E,F). In a rescue experiment, overexpression of PPARγ restored the impaired adipogenesis in NR2F6-deficient cells (Figure 5G–I). Collectively, these results suggested that NR2F6 transcriptionally activated PPARγ to promote adipocyte differentiation.

3.4. NR2F6 deletion in preadipocytes predisposes to diet-induced obesity

The aforementioned results demonstrated that loss of NR2F6 inhibited adipocyte differentiation, reduced the number of mature adipocytes, therefore promoted hypertrophy of brown adipocytes. In obesity, adipose tissues expand through either adipocyte hyperplasia or hypertrophy. As a driver for adipocyte hyperplasia, NR2F6 was significantly increased in BAT of obesity mice (Figure 6A,B). Similarly, we found NR2F6 had higher mRNA levels in iWAT and eWAT of obesity mice (Figure S7A and B). Subsequently, we compared the metabolic phenotype of WT and NR2F6-PKO mice fed HFD. NR2F6-PKO mice had significantly higher body weights as compared with WT mice under HFD (Figure 6C,D). NR2F6-PKO mice displayed lower oxygen consumption, carbon dioxide production, respiratory exchange ratio (RER) and heat during both light and dark cycles (Figure S7C–F), with similar amounts of food consumption compared with WT mice (Figure S7G), indicating that energy expenditure was decreased in NR2F6-PKO mice. The fat mass of NR2F6-PKO mice was significantly higher than WT mice (Figure 6E), whereas lean mass remained equivalent between the two groups (Figure 6F), indicating that the increased weight gain primarily resulted from increased fat accumulation. Consistently, the masses of BAT and iWAT were increased in NR2F6-PKO mice (Figure 6G,H); the BAT from NR2F6-PKO mice appeared enlarged and pale (Figure 6G,H). Moreover, the livers of NR2F6-PKO mice displayed a yellowish appearance, accompanied by a significant increase in liver mass (Figure 6G,H). H&E staining revealed a noticeable lipid accumulation in BAT and liver (Figure 6I), indicative of lipid ectopic deposition in

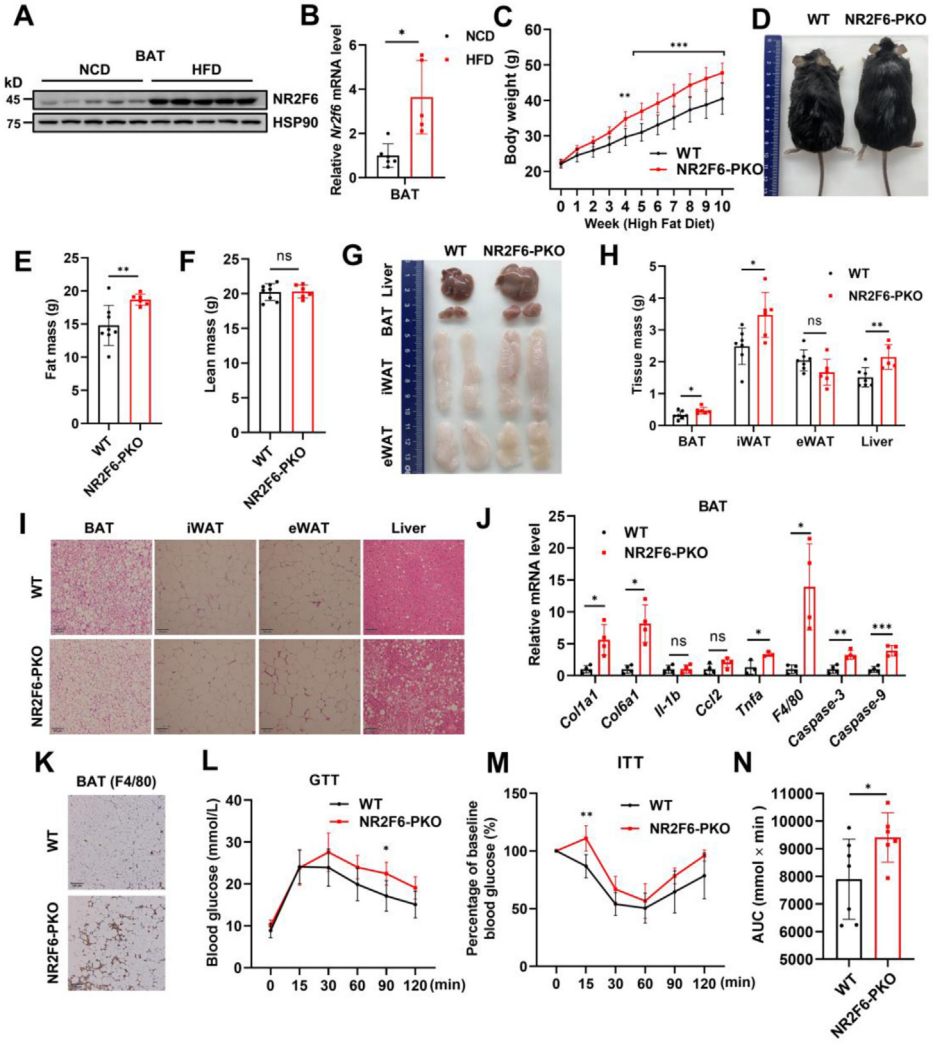

Figure 6: *Nr2f6* deletion in preadipocytes exacerbates high fat diet (HFD)-induced metabolic dysfunction. (A—B) Relative NR2F6 protein and mRNA levels in BAT of 20-week-old male C57BL/6J mice fed HFD or NCD for 12 weeks (n = 5). (C) Body weight gain of WT and NR2F6-PKO mice fed HFD (WT mice, n = 7; NR2F6-PKO mice, n = 6). (D) The photograph depicts the appearance of 20-week-old WT and NR2F6-PKO mice fed HFD for 12 weeks. (E) Fat mass of 20-week-old WT and NR2F6-PKO mice fed HFD for 12 weeks (WT mice, n = 8; NR2F6-PKO mice, n = 6). (F) Lean mass of 20-week-old WT and NR2F6-PKO mice fed HFD for 12 weeks (WT mice, n = 8; NR2F6-PKO mice, n = 6). (G) The photograph depicts gross morphology of BAT, iWAT, eWAT, and liver of 20-week-old WT and NR2F6-PKO mice fed HFD for 12 weeks. (H) The tissue mass of 20-week-old WT and NR2F6-PKO mice fed HFD for 12 weeks (WT mice, n = 7; NR2F6-PKO mice, n = 5—6). (I) H&E staining of BAT, iWAT, eWAT, and liver of 20-week-old WT and NR2F6-PKO mice fed HFD for 12 weeks. Scale bar, 100 μm. (J) Relative mRNA levels of fibrosis markers (*Col1a1* and *Col6a1*), inflammation markers (*Il-1b*, *Ccl2*, *Tnfa*, and *F4/80*) and apoptosis markers (*Caspase-3* and *Caspase-9*) in BAT of 20-week-old WT and NR2F6-PKO mice fed HFD for 12 weeks (n = 3—4). (K) F4/80 staining of BAT of 20-week-old WT and NR2F6-PKO mice fed HFD for 12 weeks. Scale bar, 100 μm. (L) Glucose tolerance test (GTT) in 18-week-old WT and NR2F6-PKO mice fed HFD for 10 weeks (WT mice, n = 7; NR2F6-PKO mice, n = 6). (M) Insulin tolerance test (ITT) in 18-week-old WT and NR2F6-PKO mice fed HFD for 10 weeks (WT mice, n = 7; NR2F6-PKO mice, n = 6). (N) Area under the curve analysis of (M) (WT mice, n = 7; NR2F6-PKO mice, n = 6). Data are represented as mean ± SD. Data in B, E, F, H, J, and N were analyzed by Student's t-test. Data in C, L, and M were analyzed by two-way ANOVA. *p < 0.05, **p < 0.01, ***p < 0.001.

NR2F6-PKO mice. While the iWAT displayed a red appearance, deletion of NR2F6 in preadipocytes did not affect the expression of thermogenic genes in iWAT of HFD-fed NR2F6-PKO mice, including *Pgc1a*, *Ucp1*, *Prdm16*, *Dio2*, and *Cidea* (Figure S7H). Furthermore, the hypertrophic BAT in NR2F6-PKO mice exhibited substantial upregulation of apoptosis markers (*Caspase-3* and *Caspase-9*) and fibrosis markers (*Col1a1* and *Col6a1*) (Figure 6J). Consistently, NR2F6 deletion promoted cell apoptosis in BAT of NR2F6-PKO mice, as shown by TUNEL staining (Figure S7I). IHC staining for F4/80 indicated increased macrophage infiltration in the BAT of NR2F6-PKO mice compared to WT mice (Figure 6K). Glucose tolerance test (GTT) and insulin tolerance test (ITT) results showed that NR2F6-PKO mice exhibited glucose intolerance and insulin resistance (Figure 6L—N). Serum insulin levels and blood glucose levels were unaltered between WT and NR2F6-PKO mice (Figure S7J and K). Additionally, the serum levels of aspartate aminotransferase (AST) and alanine aminotransferase (ALT) were relatively higher in NR2F6-PKO mice than that in the control group (Figure S7L and M), consistent with the observation of more severe fatty liver in NR2F6-PKO mice. Additionally, deletion of NR2F6 increased total cholesterol (TC) levels but not triglyceride (TG) and free fatty acid (FFA) in serum (Figure S7N—P). These data collectively suggested that loss of NR2F6 in preadipocytes caused pathologic adipose tissue remodeling and exacerbated HFD-induced metabolic dysfunction.

4. DISCUSSION

The thermogenic function of brown adipocytes relies on both the number and activity of these cells. Cold stimulation or β3 adrenergic receptor agonists activate the mitochondrial biogenesis, lipolysis and subsequent thermogenic activity in brown fat [19,26]. Additionally, they induce the proliferation of PDGFRα$^+$ brown preadipocytes and promote their differentiation [12]. Thus, the adipogenic process in brown adipocytes is critical for maintaining systemic energy balance. The development of WAT and BAT is typically regulated synergistically. Factors that promote BAT development, such as C/EBPβ and PPARγ, can also enhance WAT expansion [27]. Given the functional disparities between WAT and BAT, it is important to identify the key regulators that specifically facilitate brown fat development while leaving WAT unaffected. These regulators include PRDM16, EBF2, and Orexin [8,28–30]. The underlying mechanism behind their specific regulation of brown fat can be summarized in two aspects: first, these genes are highly enriched in brown preadipocytes, but have relatively low expression in white adipocyte lineage; second, downstream signaling pathways activated by these genes are active in brown adipocytes but absent in white adipocytes. NR2F6 aligns with the first situation, as it exhibits high expression in the brown preadipocytes but minimal expression in WAT. As a result, loss of NR2F6 hinders brown adipocyte differentiation while having little effect on white adipocytes. Targeting these genes, which specifically regulate brown adipocyte differentiation, could offer a novel strategy for metabolic disorder intervention.

Hypertrophy and hyperplasia of adipocytes are two mechanisms responsible for the expansion of adipose tissues. Defects in hyperplasia triggers adipocyte hypertrophy, which is strongly linked to metabolic disorders [3]. WAT has a unique ability to safely store excess lipids. However, ectopic lipid deposition in BAT or liver can induce insulin resistance and metabolic dysfunction. Growing evidence highlights the importance of white adipogenesis in maintaining healthy adipose tissue expansion, but the balance in hypertrophy and hyperplasia of brown adipocytes remains unclear. Here, we demonstrate that NR2F6 deficiency in brown preadipocytes inhibits adipogenesis and leads to hypertrophy of brown adipocytes, which disrupts function of brown adipocytes. Under HFD challenge, NR2F6-PKO mice are more prone to develop metabolic disorders. We label the mature adipocytes developed from PDGFRα$^+$ cells *in vivo* using R26-LSL-tdTomato model and find that loss of NR2F6 in PDGFRα$^+$ cells significantly decreases the number of mature adipocytes derived from PDGFRα$^+$ progenitors. These data indicate that NR2F6 is essential for mature adipocyte development *in vivo*. However, as we do not have the tracing model that labels NR2F6$^+$ cells, it is still unclear whether these preadipocytes exactly differentiate into mature adipocytes *in vivo*. Similarly, a recent study shows that methyltransferase-like 3 (METTL3), a key RNA methyltransferase, is enriched in BAT and is essential for brown adipogenesis. Disruption of METTL3 inhibits brown adipocyte differentiation and thereby induces hypertrophy of brown adipocytes. METTL3 deficiency restrains the thermogenic function of brown adipocytes and predisposes to HFD-induced obesity [31]. Our findings, along with others', indicate that in addition to white adipocytes, hyperplasia of brown adipocytes also actively restricts hypertrophic expansion and exhibits a protective effect against metabolic disorders. Interestingly, we observe that NR2F6-PKO mice fed HFD have an increase in iWAT but not eWAT. The cause of only an increase in iWAT remains unknown. Given these two WATs having different functions, we speculate that NR2F6 might play a different role in iWAT and eWAT. In addition, we find NR2F6-PKO mice have more apoptotic cells in BAT. At this point, we do not know which cell types are affected by apoptosis, future studies should identify specific apoptotic cells.

NR2F6 belongs to NR2F family, which consists of three different isoforms: NR2F1, NR2F2, and NR2F6. Among the NR2F family members, NR2F1 and NR2F2 exhibit the highest similarity, especially in the functionally important DNA binding domain and ligand binding domain [32]. The third member of the NR2F family, NR2F6, is more divergent but still functionally closely associated. The NR2F family members can homo- or heterodimerize with retinoid X receptor and other nuclear receptors, thereby binding to various response elements. Snail protein inhibits adipocyte differentiation by directly repressing NR2F6, which in turn increases the expression of IL-17 [33]. In addition to NR2F6, NR2F2 also plays a crucial role as a regulator of adipogenesis. NR2F2 negatively regulates the expression of Wnt10b, an inhibitor of adipogenesis, thereby promoting adipocyte differentiation [34]. NR2F2 heterozygous knockout mice display reduced adiposity, particularly decrease WAT development, and show improved glucose homeostasis [34]. All members of the NR2F family are considered orphan receptors because their endogenous ligands have not yet been identified. It is of high interest to define the factors that drive the expression of NR2F members or identify the ligands responsible for their activity in the adipogenic process.

In summary, our study reveals that NR2F6 exhibits abundant expression in the SVF of BAT. Deletion of NR2F6 in preadipocytes inhibits brown adipocyte differentiation and subsequently leads to hypertrophy and impairs function of brown adipocytes. As a result, the absence of NR2F6 aggravates HFD-induced obesity and metabolic disorders. Our findings establish NR2F6 as a novel crucial regulator of brown adipogenesis and propose targeting NR2F6 as a potential approach for maintaining metabolic homeostasis.

CREDIT AUTHORSHIP CONTRIBUTION STATEMENT

Wei-yu Zhou: Investigation. **Pei Liu:** Investigation. **Yi-fan Xia:** Investigation. **Yi-jie Shi:** Investigation. **Hong-yu Xu:** Investigation. **Meng Ding:** Investigation. **Qi-qi Yang:** Investigation. **Shu-wen Qian:** Investigation. **Yan Tang:** Investigation. **Yan Lu:** Supervision. **Qi-qun Tang:** Conceptualization, Supervision. **Yang Liu:** Conceptualization, Supervision.

ACKNOWLEDGMENTS

This work was supported by National Natural Science Foundation of China (NSFC) Grants 82370881, 82170884and 81970744 (to Y. L.), Shanghai Rising-Star Program Grants 22QA1402100 (to Y. L.), National Key R&D Program of China Grant 2018YFA0800400 (to Q.-Q. T.), the Program of Shanghai Academic Research Leader by Shanghai Municipal Science and Technology Committee (No. 21XD1423400), and funded by Peak Disciplines (Type IV) of Institutions of Higher Learning in Shanghai.

DECLARATION OF COMPETING INTEREST

The authors declare that they have no known competing financial interests or personal relationships that could have appeared to influence the work reported in this paper.

DATA AVAILABILITY

Data will be made available on request.

APPENDIX A. SUPPLEMENTARY DATA

Supplementary data to this article can be found online at https://doi.org/10.1016/j.molmet.2024.101891.

REFERENCES

[1] Sakers A, De Siqueira MK, Seale P, Villanueva CJ. Adipose-tissue plasticity in health and disease. Cell 2022;185(3):419–46.

[2] Auger C, Kajimura S. Adipose tissue remodeling in pathophysiology. Annu Rev Pathol 2023;18:71–93.

[3] Vishvanath L, Gupta RK. Contribution of adipogenesis to healthy adipose tissue expansion in obesity. J Clin Invest 2019;129(10):4022–31.

[4] Wang W, Seale P. Control of brown and beige fat development. Nat Rev Mol Cell Biol 2016;17(11):691–702.

[5] Atit R, Sgaier SK, Mohamed OA, Taketo MM, Dufort D, Joyner AL, et al. Beta-catenin activation is necessary and sufficient to specify the dorsal dermal fate in the mouse. Dev Biol 2006;296(1):164–76.

[6] Lepper C, Fan CM. Inducible lineage tracing of Pax7-descendant cells reveals embryonic origin of adult satellite cells. Genesis 2010;48(7):424–36.

[7] Burl RB, Rondini EA, Wei H, Pique-Regi R, Granneman JG. Deconstructing cold-induced brown adipocyte neogenesis in mice. Elife 2022;11.

[8] Wang W, Kissig M, Rajakumari S, Huang L, Lim HW, Won KJ, et al. Ebf2 is a selective marker of brown and beige adipogenic precursor cells. Proc Natl Acad Sci U S A 2014;111(40):14466–71.

[9] Dempersmier J, Sambeat A, Gulyaeva O, Paul SM, Hudak CS, Raposo HF, et al. Cold-inducible Zfp516 activates UCP1 transcription to promote browning of white fat and development of brown fat. Mol Cell 2015;57(2):235–46.

[10] Ohno H, Shinoda K, Ohyama K, Sharp LZ, Kajimura S. EHMT1 controls brown adipose cell fate and thermogenesis through the PRDM16 complex. Nature 2013;504(7478):163–7.

[11] Seale P, Bjork B, Yang W, Kajimura S, Chin S, Kuang S, et al. PRDM16 controls a brown fat/skeletal muscle switch. Nature 2008;454(7207):961–7.

[12] Lee YH, Petkova AP, Konkar AA, Granneman JG. Cellular origins of cold-induced brown adipocytes in adult mice. Faseb J 2015;29(1):286–99.

[13] Hermann-Kleiter N, Baier G. Orphan nuclear receptor NR2F6 acts as an essential gatekeeper of Th17 CD4+ T cell effector functions. Cell Commun Signal 2014;12:38.

[14] Klepsch V, Hermann-Kleiter N, Do-Dinh P, Jakic B, Offermann A, Efremova M, et al. Nuclear receptor NR2F6 inhibition potentiates responses to PD-L1/PD-1 cancer immune checkpoint blockade. Nat Commun 2018;9(1):1538.

[15] Olson WJ, Jakic B, Labi V, Schoeler K, Kind M, Klepsch V, et al. Orphan nuclear receptor NR2F6 suppresses T follicular helper cell accumulation through regulation of IL-21. Cell Rep 2019;28(11):2878–2891 e2875.

[16] Zhou B, Jia L, Zhang Z, Xiang L, Yuan Y, Zheng P, et al. The nuclear orphan receptor NR2F6 promotes hepatic steatosis through upregulation of fatty acid transporter CD36. Adv Sci 2020;7(21):2002273.

[17] Tang WS, Weng L, Wang X, Liu CQ, Hu GS, Yin ST, et al. The Mediator subunit MED20 organizes the early adipogenic complex to promote development of adipose tissues and diet-induced obesity. Cell Rep 2021;36(1):109314.

[18] Madisen L, Zwingman TA, Sunkin SM, Oh SW, Zariwala HA, Gu H, et al. A robust and high-throughput Cre reporting and characterization system for the whole mouse brain. Nat Neurosci 2010;13(1):133–40.

[19] Ding M, Ma YJ, Du RQ, Zhou WY, Dou X, Yang QQ, et al. CHCHD10 modulates thermogenesis of adipocytes by regulating lipolysis. Diabetes 2022;71(9):1862–79.

[20] Cui Z, Liu Y, Wan W, Xu Y, Hu Y, Ding M, et al. Ethacrynic acid targets GSTM1 to ameliorate obesity by promoting browning of white adipocytes. Protein Cell 2021;12(6):493–501.

[21] Pan D, Fujimoto M, Lopes A, Wang YX. Twist-1 is a PPARdelta-inducible, negative-feedback regulator of PGC-1alpha in brown fat metabolism. Cell 2009;137(1):73–86.

[22] Dou X, Zhou WY, Ding M, Ma YJ, Yang QQ, Qian SW, et al. The protease SENP2 controls hepatic gluconeogenesis by regulating the SUMOylation of the fuel sensor AMPKalpha. J Biol Chem 2022;298(2):101544.

[23] Liu Y, Dou X, Zhou WY, Ding M, Liu L, Du RQ, et al. Hepatic small ubiquitin-related modifier (SUMO)-Specific protease 2 controls systemic metabolism through SUMOylation-dependent regulation of liver-adipose tissue crosstalk. Hepatology 2021;74(4):1864–83.

[24] Liu Y, Ge X, Dou X, Guo L, Liu Y, Zhou SR, et al. Protein inhibitor of activated STAT 1 (PIAS1) protects against obesity-induced insulin resistance by inhibiting inflammation cascade in adipose tissue. Diabetes 2015;64(12):4061–74.

[25] Krueger KC, Costa MJ, Du H, Feldman BJ. Characterization of Cre recombinase activity for in vivo targeting of adipocyte precursor cells. Stem Cell Rep 2014;3(6):1147–58.

[26] Ding M, Xu HY, Zhou WY, Xia YF, Li BY, Shi YJ, et al. CLCF1 signaling restrains thermogenesis and disrupts metabolic homeostasis by inhibiting mitochondrial biogenesis in brown adipocytes. Proc Natl Acad Sci U S A 2023;120(33):e2305717120.

[27] Farmer SR. Transcriptional control of adipocyte formation. Cell Metabol 2006;4(4):263–73.

[28] Rajakumari S, Wu J, Ishibashi J, Lim HW, Giang AH, Won KJ, et al. EBF2 determines and maintains brown adipocyte identity. Cell Metabol 2013;17(4):562–74.

[29] Seale P, Kajimura S, Yang W, Chin S, Rohas LM, Uldry M, et al. Transcriptional control of brown fat determination by PRDM16. Cell Metabol 2007;6(1):38–54.

[30] Sellayah D, Bharaj P, Sikder D. Orexin is required for brown adipose tissue development, differentiation, and function. Cell Metabol 2011;14(4):478–90.

[31] Wang Y, Gao M, Zhu F, Li X, Yang Y, Yan Q, et al. METTL3 is essential for postnatal development of brown adipose tissue and energy expenditure in mice. Nat Commun 2020;11(1):1648.

[32] Sajinovic T, Baier G. New insights into the diverse functions of the NR2F nuclear orphan receptor family. Front Biosci 2023;28(1):13.

[33] Peláez-García A, Barderas R, Batlle R, Viñas-Castells R, Bartolomé RA, Torres S, et al. A proteomic analysis reveals that Snail regulates the expression of the nuclear orphan receptor Nuclear Receptor Subfamily 2 Group F Member 6 (Nr2f6) and interleukin 17 (IL-17) to inhibit adipocyte differentiation. Mol Cell Proteomics 2015;14(2):303–15.

[34] Li L, Xie X, Qin J, Jeha GS, Saha PK, Yan J, et al. The nuclear orphan receptor COUP-TFII plays an essential role in adipogenesis, glucose homeostasis, and energy metabolism. Cell Metabol 2009;9(1):77–87.

